pamir

10th PAMIR International Conference - Fundamental and Applied MHD
June 20–24, 2016, Cagliari, Italy

DIMENSIONALITY AND SECONDARY FLOWS IN LOW-RM MHD VORTICES.

N. Baker[1,2,3], *A. Potherat*[2], *L. Davoust*[3]

[1] *CNRS LNCMI, 38000 Grenoble, France*
[2] *AMRC Coventry University, CV15FB Coventry, UK*
[3] *Grenoble-INP / CNRS / Univ. Grenoble-Alpes, SIMaP, EPM, F-38000 Grenoble, France*

Abstract: In this paper, we examine the dimensionality of a single electrically driven vortex bounded by two no-slip and perfectly insulating horizontal walls distant by h. The study was performed in the weakly inertial limit by means of an asymptotic expansion, which is valid for any Hartmann number. We show that the dimensionality of the leading order can be fully described using the single parameter l_z^ν/h, where l_z^ν represents the distance over which the Lorentz force is able to act before being balanced by viscous dissipation. The base flow happens to introduce inertial recirculations in the meridional plane at the first order, which are shown to follow two radically different mechanisms: inverse Ekman pumping driven by a vertical pressure gradient along the axis of the vortex, or direct Ekman pumping driven by a radial pressure gradient in the Hartmann layers.

Key words: low-Rm MHD, vortex dynamics

1. Geometry and governing equations Let us consider an axisymmetric flow taking place in a cylindrical cavity of radius R. The domain is bounded by two no-slip horizontal walls located at $z = 0$ and $z = h$, and is filled with an electrically conducting fluid. A static and uniform magnetic field $B_0\,\vec{e}_z$ is applied vertically. The low-Rm approximation is assumed to hold, meaning that the magnetic field induced by the flow is negligible compared to the imposed magnetic field. In addition, the electric field $\vec{E}$ derives from the electric potential ϕ according to $\vec{E} = -\nabla\phi$. A flow is driven by injecting electric current through an electrode of radius η located on the bottom plate. The top and bottom plates are perfectly electrically insulating otherwise, which forces the current to exit the channel through the sides. Given this configuration, the electric current is known to flow radially, interacting with the vertical magnetic field to induce a patch of vertical vorticity right above the bottom Hartmann layer.

In the inertialess limit [3], the development of this patch of vorticity relies on the competition between two effects. On the one hand, the rotational part of the Lorentz force diffuses momentum along the magnetic field [2], hence leading to a vortex extending in the z direction. On the other hand, viscous friction diffuses momentum isotropically, therefore opposing the growth of the vortex along z. Calling l_z^ν the range of action of the Lorentz force, its diffusive effect takes place over the characteristic time $\tau_{2D} = (\rho/\sigma B_0^2)\,(l_z^\nu/\eta)^2$. Conversely, viscous dissipation takes place over the time $\tau_\nu = \eta^2/\nu$. Assuming a steady flow, the distance l_z^ν over which the Lorentz force is able to act before being balanced by viscous dissipation is derived by equating both effects, yielding:

$$\frac{l_z^\nu}{h} = \frac{\eta^2}{h^2}\,Ha, \tag{1}$$

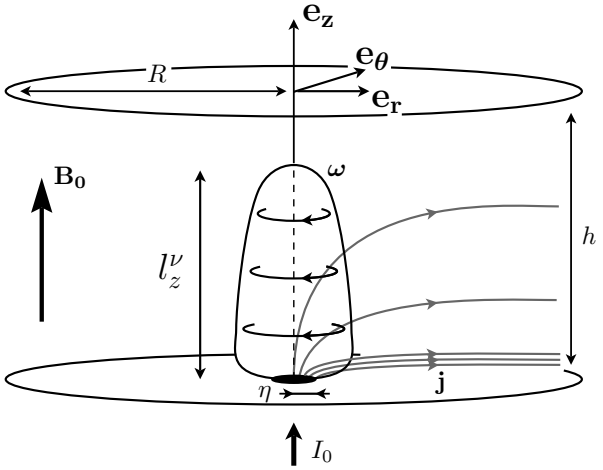

Figure 1: sketch of the problem. An isolated vortex of height $l_z^\nu < h$ confined between two horizontal no-slip and electrically insulating walls distant by h.

where $Ha = B_0 h\sqrt{\sigma/\rho\nu}$ is the Hartmann number based on the height of the channel. Asymptotically speaking, $l_z^\nu/h \ll 1$ means that the diffusive effect of the Lorentz force is balanced by viscous dissipation long before momentum can reach the top wall. In this case, the distance l_z^ν may be physically interpreted as the height of the vortex. On the contrary, $l_z^\nu/h \gg 1$ means that momentum can be diffused far beyond the top wall. This process is however blocked by the presence of the no-slip top wall, which prevents the vortex from extending past it. The ratio l_z^ν/h has been identified by [4] as the non dimensional parameter defining whether the structure is able to feel the presence of the top wall, hence controlling its dimensionality: 3D when $l_z^\nu/h \ll 1$ and quasi-2D when $l_z^\nu/h \gg 1$.

From now on, let us use the dimensionless coordinates $\tilde{r} = r/\eta$ and $\tilde{z} = z/h$, as well as the non dimensional variables $\tilde{u} = u/U$, $\tilde{\omega} = \omega\,\eta/U$, $\tilde{j} = j/\sigma U B_0$ and $\tilde{\phi} = \phi/UB_0\eta$. We also introduce the non dimensional operator $\tilde{\nabla}$ defined as

$$\tilde{\nabla} = \left(\frac{\partial}{\partial\tilde{r}}\,,\,\frac{1}{\tilde{r}}\frac{\partial}{\partial\theta}\,,\,\frac{\eta}{h}\frac{\partial}{\partial\tilde{z}}\right).$$

The governing equations consist of the steady state vorticity equation for $\tilde{\vec{\omega}} = \tilde{\nabla}\times\tilde{\vec{u}}$

$$\frac{1}{N}\left(\tilde{\vec{u}}\cdot\tilde{\nabla}\tilde{\vec{\omega}} - \tilde{\vec{\omega}}\cdot\tilde{\nabla}\tilde{\vec{u}}\right) = \frac{1}{Ha}\left(\frac{l_z^\nu}{h}\right)^{-1}\tilde{\Delta}\tilde{\vec{\omega}} + \frac{1}{\sqrt{Ha}}\left(\frac{l_z^\nu}{h}\right)^{1/2}\frac{\partial\tilde{\vec{j}}}{\partial\tilde{z}}\,, \tag{2}$$

Ohm's law

$$\tilde{\vec{j}} = -\tilde{\nabla}\tilde{\phi} + \tilde{\vec{u}}\times\vec{e}_z, \tag{3}$$

the conservation of mass

$$\tilde{\nabla}\cdot\tilde{\vec{u}} = 0, \tag{4}$$

and charge

$$\tilde{\nabla}\cdot\tilde{\vec{j}} = 0. \tag{5}$$

The problem at hand is governed by three non dimensional parameters, namely the interaction parameter N based on the width of the injection electrode η, the Hartmann number Ha based on the height of the channel h and the ratio l_z^ν/h:

$$N = \frac{\sigma B_0^2\eta}{\rho U}, \quad Ha = B_0 h\sqrt{\frac{\sigma}{\rho\nu}}, \quad \frac{l_z^\nu}{h} = \frac{\eta^2}{h^2}\,Ha. \tag{6}$$

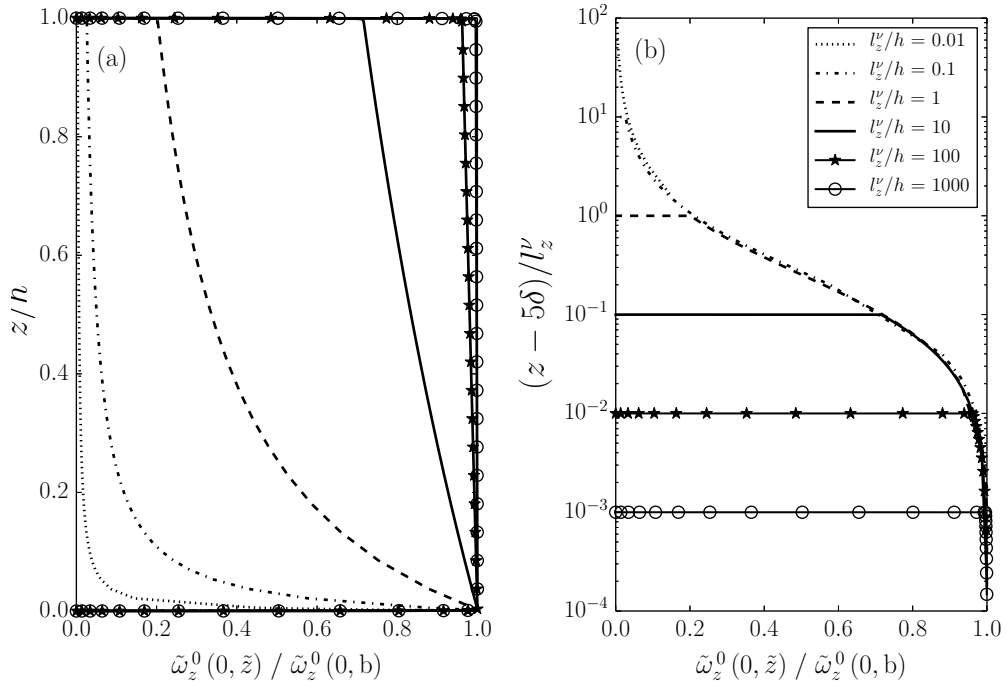

Figure 2: axial vorticity $\tilde{\omega}_{\tilde{z}}^0(0,\tilde{z})$ normalized by the vorticity right outside the bottom Hartmann layer $\tilde{\omega}_{\tilde{z}}^0(0,b)$ for $Ha = 3644$. (a): z is normalized by the height of the channel h. (b): z is normalized by the Lorentz force diffusion length l_z^ν.

The associated boundary conditions on the horizontal walls consist of no-slip boundaries, an imposed profile of vertical current at the bottom wall, and a perfectly electrically insulating top wall. In addition, we impose a perfectly conducting and free slip radial boundary. Equations (2) through (5) are solved analytically by expanding them using the regular perturbation series in the weakly inertial limit $N \gg 1$, and by looking for solutions with separated variables.

2. Results

2.1. Base flow From now on, $\tilde{\omega}_{\tilde{z}}^0(\tilde{r},t)$ and $\tilde{\omega}_{\tilde{z}}^0(\tilde{r},b)$ refer to the vorticity right outside the top and bottom Hartmann layers respectively. Figure 2 portrays the profile of vertical vorticity $\tilde{\omega}_{\tilde{z}}^0(0,\tilde{z})$ normalized by $\tilde{\omega}_{\tilde{z}}^0(0,b)$ along the axis of the channel. In figure 2.a, all structures evolve in a channel of fixed height ($\tilde{z}$ is normalized by h). This representation highlights the effect of the ratio l_z^ν/h on the dimensionality of the base flow: as l_z^ν/h increases, the momentum induced right above the injection electrode is diffused farther and farther by the Lorentz force, hence progressively smoothing out velocity gradients along $\tilde{z}$. In figure 2.b, all curves are shifted down by 5δ to account for the varying thickness of the Hartmann layer, and then normalized by l_z^ν. The collapse of all curves in these variables clearly indicates that all vortices follow a universal profile, which is solely defined by the competition between the Lorentz force and viscous dissipation. In other words, the effect of the vertical confinement is local, and only consists in ending the universal profile by introducing a no-slip boundary (the presence of the top wall is felt over a distance whose order of magnitude is no larger than the thickness of the Hartmann layer).

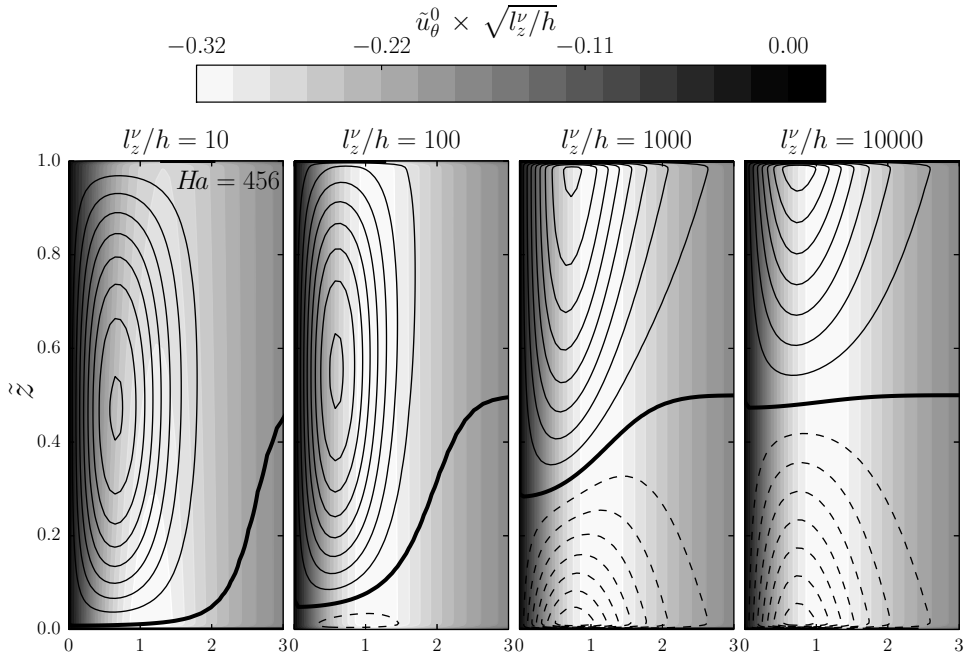

Figure 3: complete velocity field for increasingly quasi-2D base flows for $Ha = 456$. The magnitude of the base flow $\tilde{u}_\theta^0$ is indicated by filled contours. Streamlines correspond to iso-values of the stream function in the meridional plane. - - : clock-wise recirculation, —: counter-clockwise recirculation.

2.2. First order recirculations Figure 3 gives a complete view of the velocity field for increasingly 2D base flows. When the base flow is 3D ($l_z^\nu/h < 100$), a large counter-clockwise recirculation dominates the flow. This phenomenon has been observed by [5] in electrolytes, and by [6] in steady and turbulent liquid metal flows. It is driven by an axial pressure gradient that builds up along the axis of the vortex as a result of the negative gradient of azimuthal velocity along $\vec{e}_z$. Since the associated flow recirculates in opposite direction to Ekman pumping, and that both are driven by differential rotation, it was called inverse Ekman pumping by the latter authors. As the base flow becomes increasingly quasi-2D ($l_z^\nu/h > 100$), a clockwise recirculation becomes visible at the bottom of the domain, and grows steadily with l_z^ν/h. The secondary flow is then composed of two counter-rotating structures, which correspond to direct Ekman pumping, or what is also called the "tea-cup effect". Unlike inverse pumping (which stems from a pressure gradient along the axis of the vortex), direct pumping is driven by a radial pressure gradient inside the boundary layers, which develops in the bulk to oppose centrifugal forces.

The profiles of pressure gradient along the axis of the vortex are represented in figure 4 in order to illustrate the previous argument. When the flow is 3D, a positive pressure gradient exists in the bulk, whose effect is to drive a jet down along the axis of the vortex. Because this phenomenon is entirely governed by velocity gradients in the core, it is no surprise that the intensity of the inverse pumping is driven by l_z^ν/h. As a result of quasi-two dimensionality, the dependence of the pressure (or any other quantity for that matter) on $\tilde{z}$ in the bulk disappears. However, a very strong vertical pressure gradient exists at both ends of the axis as a result of a converging radial flow within the boundary layers.

3. Conclusions We showed that the dimensionality of an electrically driven vortex can be uniquely characterized by the ratio l_z^ν/h, which compares the range of action

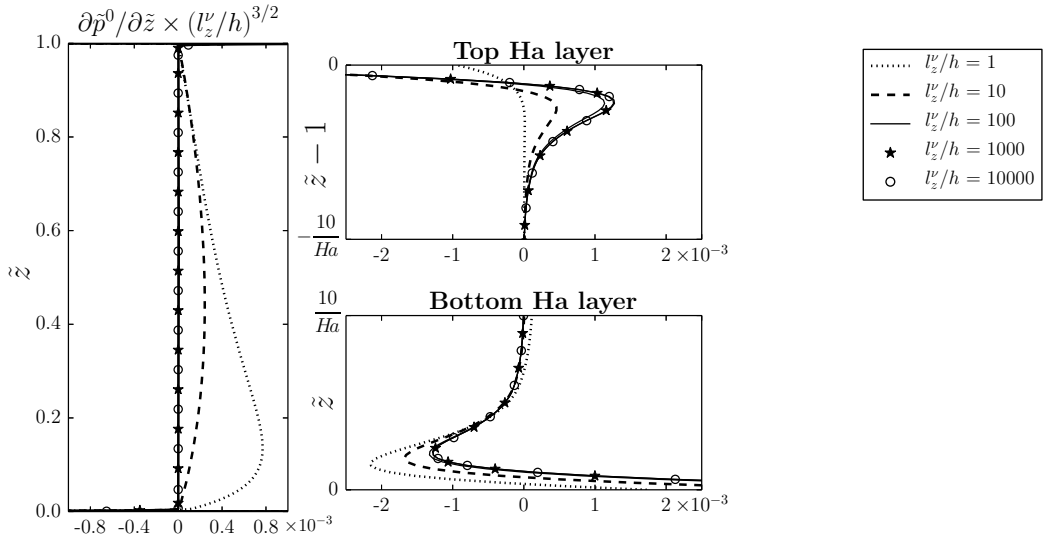

Figure 4: pressure gradient along the axis of the vortex.

of the Lorentz force to the height of the channel. Furthermore, we illustrated that two different inertial mechanisms existed to drive first order recirculations in the meridional plane: inverse and direct Ekman pumping.

REFERENCES

[1]. N. Baker, A. Potherat, and L. Davoust. Dimensionality, secondary flows and helicity in low-Rm MHD vortices. *J. Fluid Mech.*, 779, 2015.

[2]. J. Sommeria, and R. Moreau. Why, how, and when, MHD turbulence becomes two-dimensional. *J. Fluid Mech.*, 118, 1982.

[3]. K. Kalis, and Y. Kolesnikov. Numerical study of a single vortex of a viscous incompressible electrically conducting fluid in a homogeneous axial magnetic field. *Magnetohydrodynamics*, 16, 1980.

[4]. A. Potherat, and R. Klein. Why, how and when MHD turbulence at low Rm becomes three-dimensional. *J. Fluid Mech.*, 761, 2014.

[5]. R. Akkermans, A. Cieslik, L. Kamp, R. Trieling, H. Clercx, G. Van Heijst. Three-Dimensional Structure of an Electromagnetically Generated Dipolar Vortex in a Shallow Fluid Layer. *Phys. Fluids*, 20, 2008.

[6]. A. Potherat, F. Rubiconi, Y. Charles, and V. Dousset. Direct and inverse pumping in flows with homogeneous and non-homogeneous swirl. *The European Physical Journal E.*, 8, 2013.